International Journal of Machine Tools & Manufacture 49 (2009) 1096–1103

Contents lists available at ScienceDirect

International Journal of Machine Tools & Manufacture

journal homepage: www.elsevier.com/locate/ijmactool

Dynamic simulation of boring process

B. Moetakef-Imani *, N.Z. Yussefian [1]

Department of Mechanical Engineering, Ferdowsi University of Mashhad, Mashhad, Iran

ARTICLE INFO

Article history:
Received 3 November 2008
Received in revised form
10 July 2009
Accepted 16 July 2009
Available online 3 August 2009

Keywords:
Boring process
Dynamic simulation
Chatter

ABSTRACT

This article presents a model to simulate the dynamics of boring process. In boring operations the boring bar should be long and slender; therefore it is easily subjected to vibrations. Tool vibrations result in reduced tool life, poor surface finish and may also introduce chatter. Hence, predicting the vibrational behavior of boring process for certain cutting conditions and tool work-piece properties is of great importance. The proposed method models the cutting tool geometry by B-spline parametric curves. By using B-spline curves it is possible to simulate different tool geometries with a single approach. B-spline curves also enable the modeling of the kinematics of chip formation for different tool work-piece engagement conditions with a single formulation. The boring bar has been modeled by the Euler–Bernoulli beam theory. The simulation process has been implemented with MATLAB. The algorithm consists of different computational modules that are interconnected by a main program. Experimental machining tests have been conducted to verify the validity of the proposed model. Proposed dynamic models have been able to predict the dynamic cutting force components and vibration frequencies with less than 15% deviation. The proposed model has been also able to predict the chatter onset correctly.

1. Introduction

Tool or work-piece vibration in machining processes is the main limiting factor for metal removal rate and machining efficiency. In boring process due to the slenderness of boring bar, its flexibility is much more than the work-piece. Accordingly, the tool is more susceptible to vibrations. On the other hand, boring is a process that is used in finishing of precise components. Tool vibrations result in poor surface finish, reduced tool life, dimensional errors and may also introduce chatter, which is highly unfavorable. Therefore, the machining parameters should be set in a way to avoid any kind of unstable vibration during the machining process. Developing a model to simulate the machining process while the tool vibrates helps us in understanding the influence of the machining parameters on the process behavior and thereby instructs the operator to choose the optimal machining parameters for a certain boring operation. Predicting the dynamic behavior of the boring process (e.g. the dynamic cutting force components) is also necessary for designing and manufacturing of machine tool structures, tool holders and even the boring bars.

In comparison with other machining operations such as milling or turning, few researches have been conducted on the stability and dynamics of boring process. These researches can be categorized into two main groups.

The first group consists of the experimental innovations for increasing the process efficiency using passive, semi-active and active control of the machining operation without further investigation on the influence of geometrical, structural or process parameter on the boring stability. The design and manufacture of a carbon fiber epoxy boring bar with high damping coefficients [1], incorporation of a tunable vibration absorber to suppress boring vibrations [2] and employment of electrorheological fluids to control the boring bar stiffness for avoiding chatter frequency [3] are some recently proposed methods of passive, semi-active and active boring vibration control.

The second group of research tries to characterize the process behavior of a conventional boring operation across a certain range of cutting conditions. Only few researches have been conducted on the prediction of process behavior. Subramani et al. [4] introduced simple geometrical relations for cutting force computation of boring process. Empirical cutting force coefficients were used to find the cutting force components. They assumed that the boring process is orthogonal and ignored the inclination angle of the cutting edge. Later Kuster [5] developed a simulation model for the dynamics of boring process. His model did not consider the influence of rake and inclination angles. In addition, the dynamic chip load was not computed properly. Lazoglu et al. [6] used

* Corresponding author. Tel.: +98 511 8615100; fax: +98 511 8436433.
E-mail addresses: imani@ferdowsi.um.ac.ir (B. Moetakef-Imani), nima.zy@gmail.com (N.Z. Yussefian).
[1] Tel.: +1 905 5416594.

0890-6955/$ - see front matter © 2009 Elsevier Ltd. All rights reserved.
doi:10.1016/j.ijmachtools.2009.07.008

experimental cutting force components along with a modification factor to compute the dynamic cutting force during the boring process. The chip load and cutting edge contact length were found using Boolean operators between the previously meshed work-piece and the instantaneous location of the tool tip. This method could correctly predict the stability domain but the dynamic cutting force amplitudes of the predicted and measured results had noticeable deviations. In addition, their research was also confined to empirical cutting force coefficients, which were derived for a certain pair of cutting tool and work-piece. Budak and Ozlu [7] proposed a stability analysis model for boring and turning operations, but dynamic cutting force simulation was not taken into consideration. In a recent study, Yussefian et al. [8] proposed a comprehensive model for simulating the mechanics of boring process. The model consists of a novel geometrical approach that employs B-spline curves to simulate the machining process. It also presents a new force model for predicting the cutting force of machining with nose radius tools.

This research extends the previously proposed model to simulate the dynamic behavior of the boring process. The presented approach employs B-spline and their specific features for the geometrical modeling of the machining process. Advanced curve intersection methods are used to find the instantaneous chip boundary and thereby compute the instantaneous chip load. The boring bar vibration is modeled by the Euler–Bernoulli beam equation. The model aims to describe the vibrational behavior of the boring process for a certain range of machining parameters.

Henceforth the paper is organized as follows. In the second section, an introduction to the self-excited vibration is presented. The boring bar equation of motion is then modeled using the Euler–Bernoulli beam theory. In Section 3 the kinematics of chip-load formation is modeled by B-spline parametric curves. Section 4 describes the dynamic simulation methodology using MATLAB programming. Section 5 explains the experimental machining tests and compares the simulated and experimental results.

2. Tool vibrations

The machine, cutting tool and work-piece form a structural system with complex dynamic characteristics. Under certain conditions this system may undergo excessive vibrations [9].

2.1. Types of vibrations

Vibrations in machine tool structures can be generally categorized into three main groups:

Free or transient vibrations: Free vibrations in machine tools occur almost in every machining operation. The vibrations due to the initial engagement of the tool and work-piece or the vibrations caused by the rapid reciprocal motion of the machine tool table are some sorts of transient vibrations. The machine tool vibrates in its natural modes until the vibration is damped.

Forced vibration: Forced vibrations occur when a periodic force is applied to the machine tool structure. The engagement of multi-insert tools in the cut and the run-out of the tool tip are the two main sources of forced vibrations. Also, there exist other sources like the vibrations transmitted to the machine tool by its foundation from the nearby machinery. The system vibrates in the actuating frequency and if this frequency coincides one of the system's natural frequencies the resonance occurs.

Self-excited vibration: The most important type of vibration in machining processes is self-excited vibration. When the tool initially engages the cut, it undergoes transient vibrations. If machining parameters like depth of cut, feed rate and cutting speed are not set properly, transient vibration may lead to

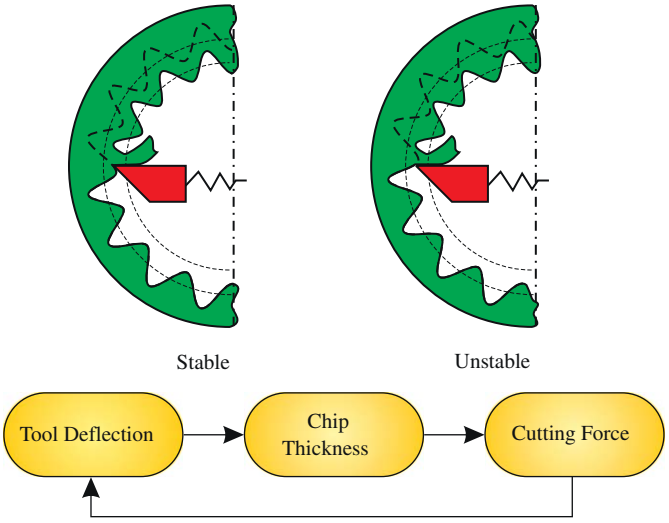

Fig. 1. Regenerative chatter mechanism in boring operation.

self-excited or chatter vibrations. If the tool vibrates, the chip thickness will change from its nominal value. The variation of chip thickness results in the oscillation of cutting force magnitude. The new cutting force will impose a new deflection to the cutting tool. Consequently, the interaction of cutting force, tool deflection and chip thickness forms a loop (Fig. 1). If machining parameters and structural characteristics of the machine tool structure are not maintained accordingly, chatter occurs and unstable vibrations will commence (Fig. 1). As a result, the vibration amplitude increases by every tool pass during the machining process. This continues until the tool or the work-piece or one of power transmitting components fail, unless a limiting factor (like the jump out of the cut of the tool) confines the vibration amplitude.

2.2. Equation of motion

In boring process the boring bar is more flexible than the work-piece; thus the most flexible component is the tool. The boring bar is much stiffer in torsion than in bending [10]. Hence, in the analysis of boring bar vibrations, the bending modes of radial and tangential directions should be taken into account. On the other hand, it is known by geometrical considerations that the boring bar deflections in tangential direction (Z) do not affect the chip thickness [6]. Therefore, the boring bar can be modeled as a cantilever beam vibrating in the radial (DOC) direction, Fig. 2. Most of the previously proposed models for boring bar vibrations rely on modeling the boring bar equation of motion by lumped parameters [4–7]. However, modeling a distributed system of boring bar consisting of infinite number of modes with lumped parameters brings future potential problems [10]. A reasonable model for boring bar is an Euler–Bernoulli beam with clamped free boundary conditions. The Euler–Bernoulli beam differential equation describing the transverse motion in radial (Y) direction is expressed by [11]

$$\rho A_b \frac{\partial^2 y(x,\ t)}{\partial t^2} + \frac{\partial^2}{\partial x^2}\left[EI(x)\frac{\partial^2 y(x,\ t)}{\partial x^2}\right] = f(x,\ t) \tag{1}$$

where ρ is the boring bar density, A_b is the boring bar cross-sectional area, EI the flexural stiffness and $f(x, t)$ the force per unit length of the bar.

It is assumed that both the cross-sectional area and flexural stiffness are constant along the bar. If normal modes of the system $\Phi_n(x)$ are known, its deflection at any point x along the beam can

be evaluated by [11]

$$y(x,\ t) = \sum_{n=1}^{\infty} q_n(t)\phi_n(x) \tag{2}$$

where $q_n(t)$ is generalized coordinate or modal participation coefficient and must satisfy the following condition:

$$\frac{d^2q_n(t)}{dt^2} + 2\zeta_n\omega_n\frac{dq_n(t)}{dt} + \omega_n^2 q_n(t) = \int f(x,\ t)\phi_n(x)dx \tag{3}$$

For a constant concentrated force Eq. (3) will convert to

$$\frac{d^2q_n(t)}{dt^2} + 2\xi_n\omega_n\frac{dq_n(t)}{dt} + \omega_n^2 q_n(t) = F\phi_n(a) \tag{4}$$

where a is the location of the applied force. The solution to the boundary conditions yields the characteristic equation of $\cos(\beta L)\cosh(\beta L) = -1$. β_n are the eigen values of the characteristic equation and for the three first modes can be evaluated by

$$\beta_n = \left\{\frac{1.8752}{L},\ \frac{4.6941}{L},\ \frac{7.8548}{L}\right\} \tag{5}$$

The theoretical natural frequencies of the boring bar are expressed by

$$f_n = \frac{\beta_n}{2\pi}\sqrt{\frac{EI}{\rho A_b}} \tag{6}$$

The normal modes $\phi_n(x)$ can be computed by substituting the beam boundary conditions as follows:

$$\phi_n(x) = \lambda_n[\cosh(\beta_n x) - \cos(\beta_n x) - \mu_j(\sinh(\beta_n x) - \sin(\beta_n x))] \tag{7}$$

$$\mu_n = \frac{\cosh(\beta_n) + \cos(\beta_n)}{\sinh(\beta_n) + \sin(\beta_n)} \tag{8}$$

λ_n is the normalizing coefficient of the nth mode and must satisfy

$$\int_0^L \rho A_b \phi_n^2(x)dx = 1, \quad j = 1,\ 2\ldots \tag{9}$$

In addition to four boundary conditions that are determined by cantilever beam end conditions, two initial conditions are also needed to solve Eq. (2) which are as follows:

$$y(x,\ t=0) = \sum_{n=1}^{\infty} q_n(0)\phi_n(x) = y_0(x)$$
$$\frac{\partial y}{\partial t}(x,\ t=0) = \sum_{n=1}^{\infty} q_n'(0)\phi_n(x) = V_0(x) \tag{10}$$

where $q_n(0)$ and $q'_n(0)$ can be computed by

$$q_n(0) = \int_0^l \rho A(x)\phi_n(x)y_0(x)dx$$
$$q_n'(0) = \int_0^l \rho A(x)\phi_n(x)V_0(x)dx \tag{11}$$

2.3. Modified Euler–Bernoulli beam equation

The Euler–Bernoulli model of the boring bar overestimates the actual bar first resonance frequencies. The first reason for this is the fact that the Euler–Bernoulli beam model considers the clamping condition rigid while the clamping applied by clamping bolts in an actual bar fixture is not infinitely rigid. Secondly, since the Euler–Bernoulli beam model ignores the effects of shear deformation and rotary inertia, the boring bar Eigen frequencies will be slightly overestimated [12,13]. In order to compensate for the flexibility in the clamping condition, and thereby correlate the natural frequency of the Euler–Bernoulli beam model with that of an actual boring bar, a method similar to the one proposed by Andren et al. [12] is employed. For this, the theoretical bar should be considered longer than the actual boring bar. The modified bar length can be found by measuring the first resonance frequency by the impact test method. Having the first resonance frequency, the modified length of the bar can be evaluated by Eq. (6).

Table 1 illustrates the dynamic properties of the boring bar used in the current research along with the computed values of modified bar lengths. Damping ratio has also been computed by the impact test.

It should be noted that this method compensates a portion of the natural frequency overestimation by the Euler–Bernoulli beam theory.

Table 1
Dynamic properties of boring bar.

L_e (m)	L (m)	ξ_y	w_{1y} (Hz)	Parameter
0.1535	0.14	0.025	620	Value

3. Kinematics of chip-load formation

The cutting edge has been interpolated by a third degree clamped B-spline with uniform parametization and knot vector [14]. The cutting edge equation can therefore be expressed by

$$c_x^j(u) = N(u)\,P_x$$
$$c_y^j(u) = N(u)\,P_y \tag{12}$$

where $N(u)$ and P are B-spline basis functions and B-spline control points, respectively. u is the B-spline parameter that belongs to [0, 1].

In order to model the instantaneous tool location, work-piece is divided into a number of angular elements, Fig. 2. As the work-piece revolves with the spindle speed, the cutting edge engages these elements consecutively. In any element, the instantaneous cutting edge equation can be found using the B-spline parametric curves translation property [14]:

$$c_x^{k,\,j}(u,\ t) = N(u)[P_x - j\,c]$$
$$c_y^{k,\,j}(u,\ t) = N(u)[P_y + y(t)] \tag{13}$$

where c is feed per revolution and $y(t)$ is the deflection in radial direction (see Fig. 3).

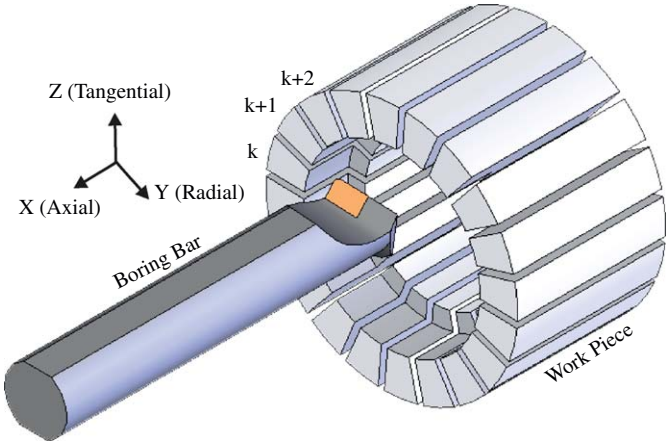

Fig. 2. The meshing of work-piece into angular elements.

When the tool does not vibrate the chip load can be found by considering two successive cutting edge locations [8]. It should be noted that four different chip configurations can be identified depending on the values of depth of cut (DOC), feed rate (c) and also the tool nose radius (r) [15].

Due to the tool vibration, the chip load varies as a function of machining parameters, tool edge geometry and structural properties of the boring bar. In order to include the effect of regeneration, three successive locations of the cutting edge have been taken into account. Depending on machining parameters, cutting edge geometry and instantaneous deflection of the tool tip, five different vibrational configurations can be identified, Fig. 4 As can be seen in Fig. 4, case 5 represents the condition at which the amplitude of vibration is in such a way that the tool jumps out of the cut. It is obvious that for this case the chip load on the cutting edge is zero; consequently, the cutting force components vanish. For the remaining four configurations the tool is engaged in the cut. Combining these four vibrational configurations with four chip configurations results in the identification of sixteen different conditions of tool and work-piece dynamic engagement. It should be noted that during a machining experiment the actual depth of cut (DOC) and feed rate (c) change as a function of the tool deflection. Consequently, depending on the instantaneous values of DOC and c with respect to the tool nose radius value (r), any of these sixteen conditions can be the case of tool and work-piece engagement. For each tool work-piece engagement condition the geometry of the chip load differs. This is designated by the shaded area (current cut) in Fig. 4.

In order to determine the chip boundary the intersection points of the current cutting edge location, the last effective cutting edge location and the DOC marginal line should be found, Fig. 5. This is done by an analytic parametric curve intersection method; further details can be found in [8]. Once the chip boundaries have been determined, for any tool work-piece engagement condition the instantaneous chip load and cutting edge contact length can be computed by

$$A_t^{k,j} = \int_{u_{st}^{k,j}}^{u_{\text{int}}^{k,j}} C_y^{k,j}(u)\frac{dC_x^{k,j}(u)}{du}du - \int_{u_{st}^{k,p}}^{u_{\text{int}}^{k,p}} C_y^{k,p}(u)\frac{dC_x^{k,p}(u)}{du}du - \sum_{i=1}^{q} A_t^{k,j-q} \tag{14}$$

$$L_t^{k,j} = \int_{u_{st}^{k,p}}^{u_{\text{int}}^{k,j}} \sqrt{\left[\frac{dC_x^{k,j}(u)}{du}\right]^2 + \left[\frac{dC_y^{k,j}(u)}{du}\right]^2}\,du \tag{15}$$

where u_{st} and u_{int} are the corresponding parameters of the first and the last points of the cutting edge that are engaged in the cut, respectively. p is the number of the last effective cutting pass and q defines the total number of intermediate chip loads between the current and last effective cutting edge. The values of p and q

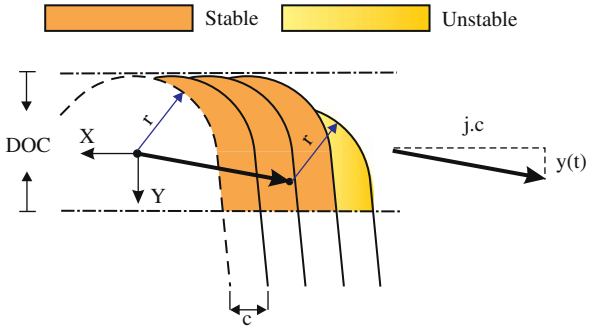

Fig. 3. Instantaneous cutting edge location.

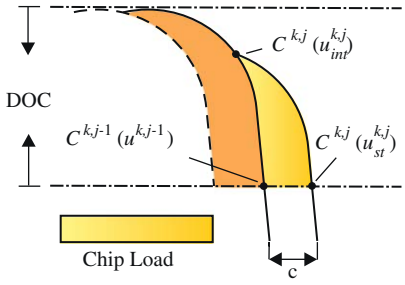

Fig. 5. Dynamic chip boundary and chip-load computation (Case 1).

Table 2
Values of the parameters p and q of Eqs. (14) and (15).

Configuration	1	2	3	4
p	$j-1$	$j-2$	$j-3$	$j-3$
q	0	1	2	2

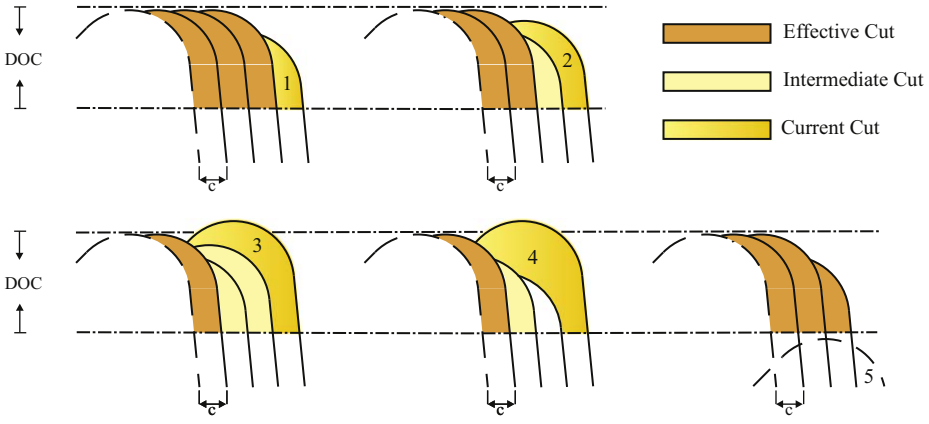

Fig. 4. Different vibrational configurations.

depend on the vibrational configuration (Fig. 4) and are listed in Table 2.

It should be noted that B-spline parametric curves not only facilitate the modeling of the complicated tool work-piece interaction during a dynamic machining process with a single approach but also enable the modeling of different cutting edge geometries.

4. Dynamic simulation

Having found the cutting edge contact length and the chip load, the instantaneous cutting force components are computed using the previously proposed method, see [8] for details. It should be pointed out that due to the employment of B-spline parametric curves, the previously proposed force model remains valid for the condition that there exist tool deflections [8]. Orthogonal cutting force coefficients were used to correlate the chip-load geometry to the cutting force components. Once the dynamic chip flow angle and cutting force components are known, the tool deflection can be computed by Eq. (1). It should be noted that the computed end beam deflection and velocity at the previous work-piece element are taken as the initial conditions of Eq. (1), that is

$$y^{k,j}(x,\ 0) = y^{k-1,\ j}(x,\ \Delta t)$$

$$V^{k,j}(x,\ 0) = \frac{\partial y^{k,j}}{\partial t}(x,\ 0) = V^{k-1,j}(x,\ \Delta t) \tag{16}$$

where Δt is the time step of the simulation process and depends on the spindle speed and the number of work-piece elements. The newly computed deflection is then used to find the new cutting edge engagement condition and the instantaneous chip load in the succeeding work-piece element.

Based on the above-mentioned approach, the algorithm of the dynamic simulation of the boring process is implemented in MATLAB. The algorithm contains different computational modules, which can be classified as follows:

- The module of geometrical simulation of the cutting edge using B-spline parametric curves.
- The module of chip boundary determination using advanced parametric curve intersection approaches.
- The chip load and cutting edge contact length computation module.
- The dynamic chip flow angle and dynamic cutting force components computations module.
- The boring bar vibration simulation module.

Fig. 6 illustrates the flow chart of the proposed algorithm for the dynamic simulation of boring process.

5. Results and discussion

A boring bar with 20 mm diameter and 140 mm length ($L/D = 7$) is used to implement the machining tests. The carbide inserts with 0.4 mm nose radius and flat rake face are used to machine the aluminum 6061 tubes. The geometrical properties of the cutting tool are presented in Table 3.

In order to validate the proposed method, 30 boring experiments were conducted. The cutting speed, feed rate and radial depth of cut were in the range of 70–110 [m/min], 0.08–0.24 [mm/rev] and 0.2–4 [mm], respectively. Cutting force components are measured in three orthogonal directions by a KISTLER 9255b dynamometer. The dynamic simulation program was also implemented for every corresponding machining experiment. For the sake of comparison between the experimental measurements and numerical simulations, two different cutting tests will be presented. The cutting conditions for these two cutting experiments are reported in Table 4. The depth of cut (DOC) is set to 0.5 and 4 mm for tests A and B, respectively. All other conditions for these tests are equal.

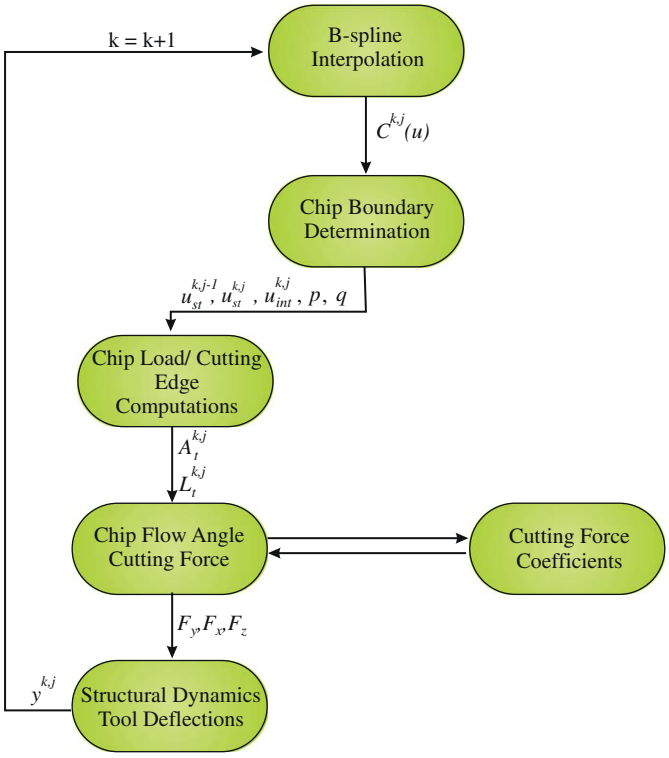

Fig. 6. The algorithm for dynamic simulation of boring process.

Table 3
Geometrical specifications of the cutting tool.

Parameter	L (m)	r (mm)	α_s (deg.)	α_b (deg.)	c_s (deg.)	c_e (deg.)
Value	0.14	0.4	−5	0	−3	32

Table 4
Geometrical specifications of the cutting tool.

Parameter	DOC (mm)	c (mm/rev)	V (m/min)	D0 (mm)	Result
Test A	0.5	0.14	95	30.5	Stable
Test B	4	0.14	95	30.5	Chatter

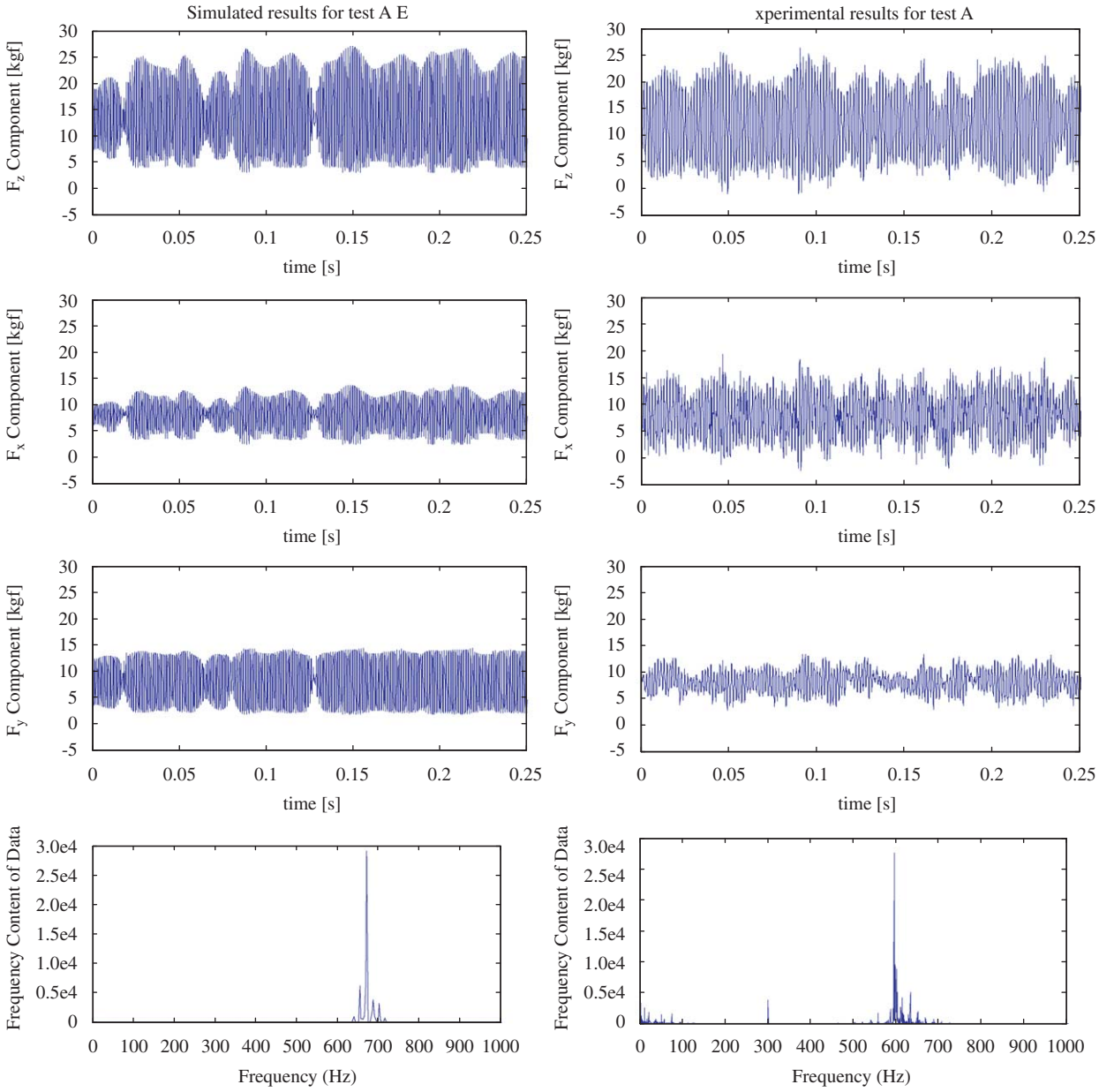

Fig. 7. Experimental and simulated cutting force values for test A.

Table 5
Comparison of experimental values of cutting force components for test A.

	F_y (kgf)	F_x (kgf)	F_z (kgf)
Simulated mean value	7.35	8.23	13.68
Measured mean value	8.08	8.09	12.18
Simulated [min, max]	[2.27,13.85]	[3.45,12.45]	[4.08,24.08]
Measured [min, max]	[3.97,12.45]	[0.20,16]	[1.01,23.60]

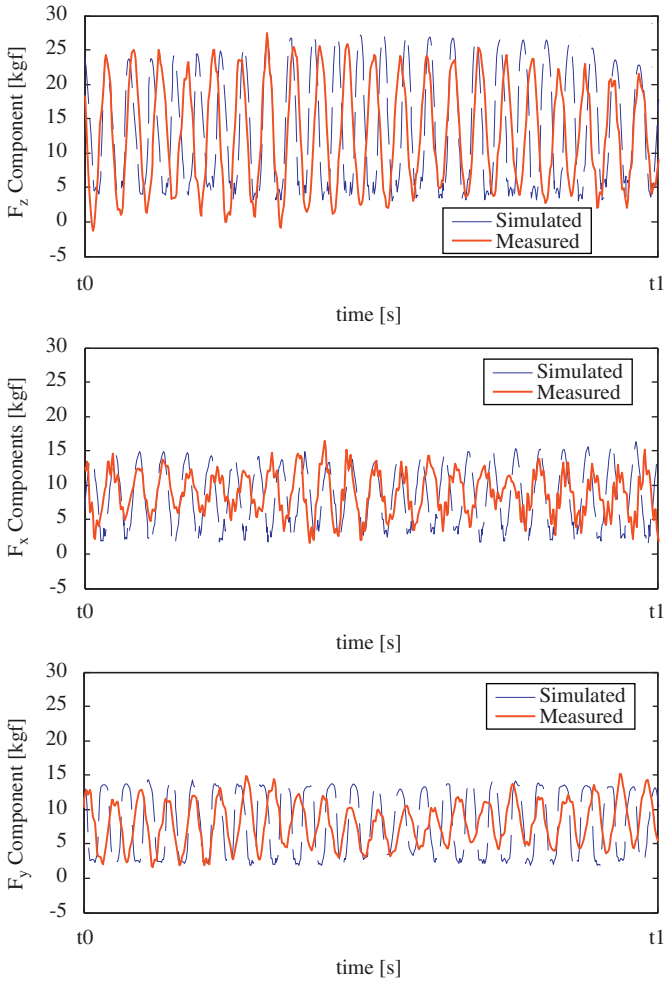

Fig. 8. Comparison of experimental and simulated cutting force components, Test A.

5.1. Test A

Measured and predicted cutting force components for boring with machining conditions of test A are depicted in Fig. 7. When the tool first engages the cut, it undergoes transient vibrations. But after several revolutions, the cutting process becomes stable and the tool continues to vibrate periodically with relatively constant amplitude. So the condition of test A is stable and chatter-free cutting machining operation. The simulated peak frequency occurs at 672 Hz with a deviation of 12.94% above the measured value of 594 Hz. This deviation results from the overestimation of the Eigen frequencies by the Euler–Bernoulli beam equation. Table 5 compares the results of cutting force components measurement by a dynamometer with the simulation results by the proposed algorithm. As can be seen in the table the measured values of the cutting force components in x, y and z direction have been predicted by 9%, 2% and 12% errors in magnitude. This amount of error is consistent with the validity interval of $\pm 10\%$ for the cutting force computation [8], which could be due to the cutting force coefficient computations.

Fig. 8 illustrates the enlarged view of the measured and predicted cutting force components. As can be seen, the proposed model predicts the cutting force components with good agreement.

5.2. Test B

Experimental and simulated cutting force components in time domain for the condition of test B are shown in Fig. 9. It was observed from the measured data that the machining process was unstable with chattering frequency around 573 Hz. In case of chatter, measured force components oscillate randomly and grow rapidly to large amplitudes. It is obvious from Fig. 9 that the simulated results had also predicted the incidence of chatter vibrations. Although the model was capable of truly predicting the chatter occurrence for the conditions of test B, the variation of simulated and measured cutting force amplitudes is increased. This is due to the fact that the measured cutting force components have been amplified by chatter frequency [6]. As a consequence of high vibration amplitudes, the actual geometrical angles of the cutting tool will change from their nominal values. It is well known that the variation of cutting tool angles will affect the cutting force components significantly [8,16]. The high reciprocating velocity of the tool tip makes the cutting process be accompanied with the plunging of the tool into the work-piece. The high acceleration of the tool increases the effect of the tool inertia forces on dynamometer measurements. All of these will make the prediction of dynamic characteristic of the process under chatter vibration almost impossible. However, for any dynamic model the correct prediction of chatter onset is enough since no practical machining operation will be carried out under chatter conditions.

6. Conclusions

In this research a model is presented to simulate the dynamics of boring process. The proposed approach relies on the novel algorithms of geometrical modeling. In contrast to the previous models that were only able to predict the stability region, this model computes the dynamic cutting force components and frequencies in stable boring operation. The performed cutting experiments have shown that the cutting force components and the vibration frequencies in chatter-free dynamic boring operation could be predicted within $\pm 15\%$ error margin. The model is valid for both finishing (DOC $< r$) and roughing (DOC $> r$) boring processes. The model is also able to predict the chatter onset in boring operation.

Due to the nonlinear geometry of the edge, the influence of depth of cut and feed rate is interrelated and should not be separately investigated. The instantaneous chip load is computed to incorporate the effect of depth of cut and feed rate. The influence of geometrical properties (like tool angles and nose radius) as well as structural and process parameters could be investigated using this model. The stability and efficiency of the process depends on the combined effect of all these parameters.

The proposed model provides a better understanding of a certain boring process. By using this method, a multivariate analysis could be performed to obtain the optimal geometrical, structural or machining process parameters. The proposed method could also be employed for machine tool, boring bar and tool holder design where a better understanding of the operational vibration frequencies and cutting force amplitudes is a necessity.

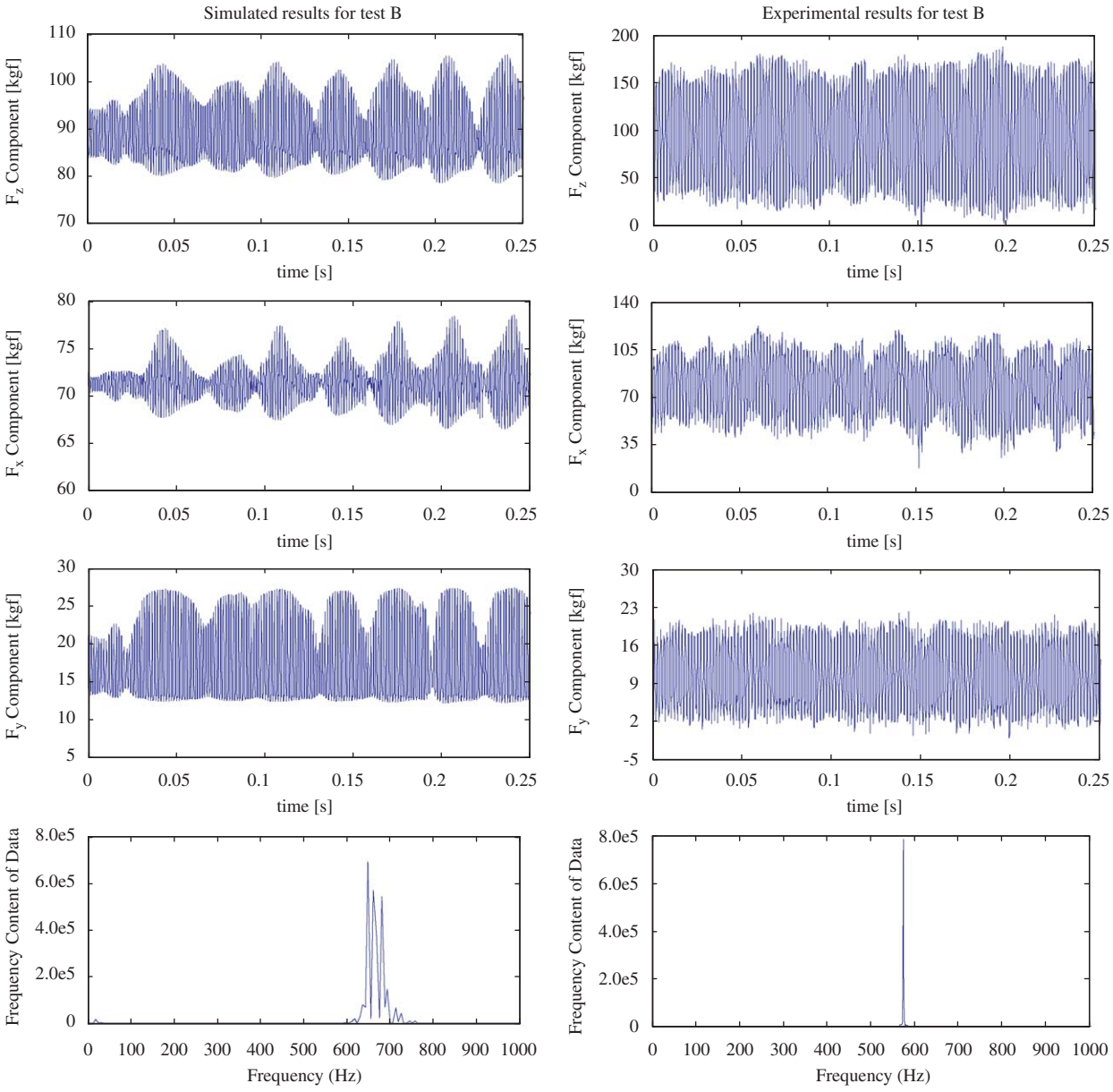

Fig. 9. Experimental and simulated cutting force values for test B.

References

[1] Dai Gil Lee, Hui Yun Hwang, Jin Kook Kim, Design and manufacture of a carbon fiber epoxy rotating boring bar, Composite Structures 60 (2003) 115–124.

[2] H. Moradi, F. Bakhtiari-Nejad, M.R. Movahhedy, Tunable vibration absorber design to suppress vibrations: an application in boring manufacturing process, Journal of Sound and Vibration 318 (2008) 93–108.

[3] Min Wang, Renyuan Fei, Chatter suppression based on nonlinear vibration characteristic of electrorheological fluids, International Journal of Machine Tools & Manufacture 39 (1999) 1925–1934.

[4] G. Subramani, R. Suvada, S.G. Kapoor, R.G. DeVor, W. Meingast, A model for the prediction of force system for cylinder boring process, in: Proceedings of the XV NAMRC, 1987, pp. 439–446.

[5] F. Kuster, Cutting dynamics and stability of boring bars, Annals of CIRP 56 (1) (2007) 401–404.

[6] I. Lazoglu, F. Atabey, Y. Altintas, Dynamics of boring processes: Part III—time domain modeling, International Journal of Machine Tools Manufacture 42 (2002) 1567–1576.

[7] E. Budak, E. Ozlu, Analytial modeling of chatter stability in turning and boring operations: a multi-dimensional approach, Annals of the CIRP 56 (2007) 401–404.

[8] N.Z. Yussefian, B. Moetakef-Imani, H. El-Mounayri, The prediction of cutting force for boring process, International Journal of Machine Tools and Manufacture 48 (2008) 1387–1394.

[9] Sandvik Coromant, Technical Editorial dept. Modern Metal Cutting A Practical Handbook, First edition, 1994, ISBN 91-97 22 99-0-3.

[10] C. Mei, Active regenerative chatter suppression during boring manufacturing process, Robotics and Computer-Integrated Manufacturing 21 (2005) 153–158.

[11] S.S. Rao, Vibration of Continuous Systems, John Wiley & Sons, 2007, ISBN: 77171-5.

[12] L. Andren, L. Hakansson, A. Brandt, I. Claesson, Identification of motion of cutting tool vibration in a continuous boring operation—correlation to structural properties, Mechanical Systems and Signal Processing 18 (2004) 903–927.

[13] Henrik Akesson, Tatiana Smirnova, Thomas Lago, Lars Hakansson, Analysis of Dynamic Properties of Boring Bars Concerning Different Clamping Conditions, Blenkige Institute of Technology, Research Report 2007:6, ISSN: 1103-1581.

[14] L. Piegl, W. Tiller, The NURBS Book, Springer, New York, 1997, ISBN 3-540-61545-8.

[15] F. Atabey, I. Lazoglu, Y. Altintas, Mechanics of boring processes—Part I, International Journal of Machine Tools and Manufacture 43 (2003) 463–476.

[16] R. Komanduri, M. Lee, L.M. Raff, The significance of normal rake in oblique machining, International Journal of Machine Tools & Manufacture 44 (2004) 1115–1124.